Non-isothermal crystallization of biodegradable polymer (MaterBi)/ polyolefin (PP)/hemp fibres ternary composites

C. J. Perez & V. A. Alvarez

Journal of Thermal Analysis and Calorimetry
An International Forum for Thermal Studies

ISSN 1388-6150
Volume 120
Number 2

J Therm Anal Calorim (2015)
120:1445-1455
DOI 10.1007/s10973-014-4368-0

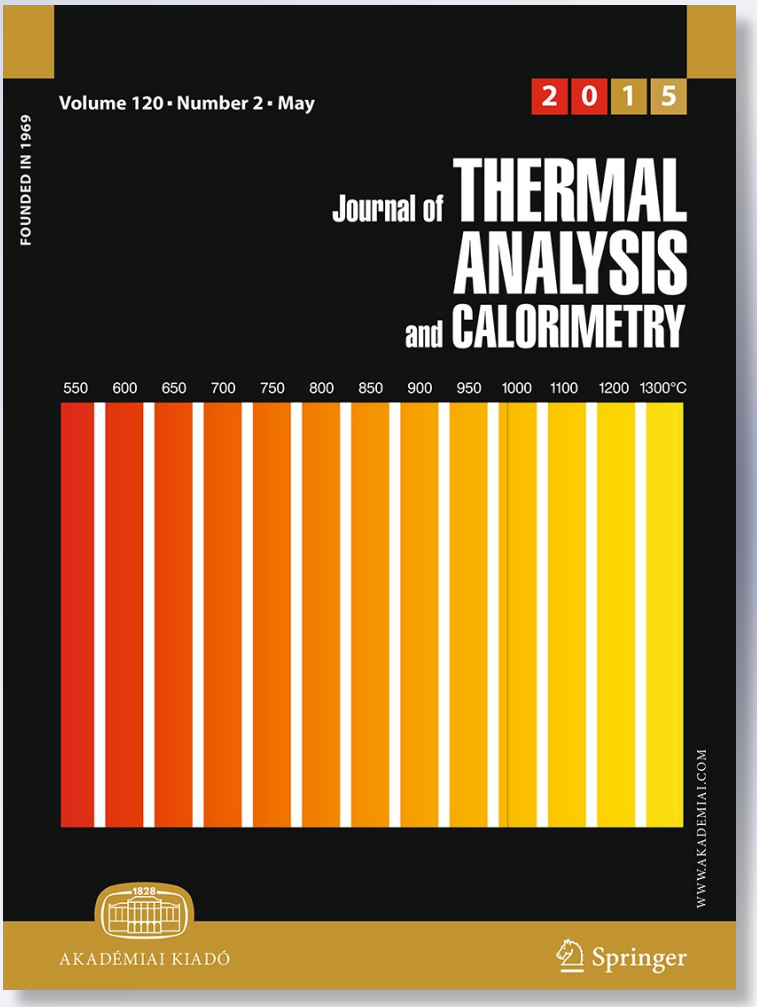

Springer

J Therm Anal Calorim (2015) 120:1445–1455
DOI 10.1007/s10973-014-4368-0

Non-isothermal crystallization of biodegradable polymer (MaterBi)/polyolefin (PP)/hemp fibres ternary composites

C. J. Perez · V. A. Alvarez

Received: 24 October 2014 / Accepted: 19 December 2014 / Published online: 28 January 2015

Abstract The non-isothermal crystallization of biodegradable thermoplastic matrix (Mater-Bi®, MB) and traditional thermoplastic (polypropylene, PP) blends was studied using differential scanning calorimetry (DSC). Hemp fibres were used as filler, and maleic anhydride functionalized polypropylene (PP*) was employed as compatibilizer. MB forms immiscible blends with PP. Both, molten MB act as nucleating agent enhancing the crystallization rate of PP and the solidified PP act as nucleating agent to enhance the crystallization of MB. The values of half-time of crystallization ($t_{1/2}$) and the parameter Z_c, from Avrami's method which characterize the kinetics of non-isothermal crystallization, showed that the crystallization rate, at the same cooling rate, decreased with the fibres and increased with the PP*; showing the retarding and accelerating effects, respectively. Some models, such as the Liu-Mo and Avrami, were found to provide a fairly satisfactory description of the crystallization kinetics of the studied blends. These results are further supported by the effective activation energy calculations by iso-conversional method of Friedman.

C. J. Perez
Polymer Science and Engineering Group, Research Institute of Material Science and Technology (INTEMA), National University of Mar del Plata (UNMdP), Av. Juan B. Justo 4302, 7600 Mar Del Plata, Argentina

V. A. Alvarez (✉)
Composite Materials Group (CoMP), Research Institute of Material Science and Technology (INTEMA), National University of Mar del Plata (UNMdP), Solís 7575, 7600 Mar Del Plata, Argentina
e-mail: alvarezvera@fi.mdp.edu.ar

Keywords Non-isothermal crystallization · Polypropylene · Biodegradable polymer · Polycaprolactone–starch blends · Natural fibres

Introduction

The amount of plastic in municipal waste streams was equal to the combined amount of metal and glass. Biodegradable materials made from renewable resources have been tested as alternatives to petroleum-based plastics [1]. Biodegradable polymers constitute a new family of polymers designed to be degraded by living organisms. They offer a possible alternative to traditional non-degradable polymers when recycling is impractical or not economical, and they can be composted together with food and yard waste [2, 3]. Most of biodegradable polymers are unsuitable for packaging applications due to several disadvantages, mainly: brittleness in the absence of plasticizers; poor water resistance and deterioration of mechanical properties upon exposure to environmental conditions (both last related with the hydrophilic nature of components).

It is known that because of their excellent processing and final properties together with its low costs, polyolefins, such as polypropylene have occupied a special status as commodity plastics. The significant annual growth of these plastics when used as packaging materials has imposed a colossal waste disposal problem for municipal sewage treatment plants. The major drawback of such packaging plastics is that they are non-biodegradable.

Different strategies have been investigated in order to find biodegradable materials with acceptable ranges of final properties and possibilities to process them in the traditional way; nevertheless, each one has advantageous and drawbacks and so the search for a "green" solution is still under investigation. One alternative is the development of

partially biodegradable polymers based on polyolefins, blending a biodegradable material with a polyolefin [4, 5]. One advantageous possibility is to develop blends of biodegradable polymers with traditional ones to obtain materials with improved cost/performances ratio.

Regarding biodegradation, the intention of blending a biodegradable polymer with a traditional one is that after disposal, degradation of biodegradable material in the blend would create voids and to weak the integrity of the polyolefin [5, 6].

In order to avoid the loss in mechanical properties in these kinds of mixtures, the use of fibres is a good alternative [7]. Natural fibres exhibit several advantages as reinforcement of biodegradable polymer: biodegradability, low density, high specific properties, low cost, nonabrasive processing characteristics and extended availability from renewable resources [8, 9]. Additionally, in this kind of composites, the fibre-matrix can be improved by employing chemical treatments of fibres and/or polymers [10–12]. In such line, Ul Haque et al. [7] have prepared and characterized ternary biodegradable polymer/conventional polymer/chemically treated hemp systems; nevertheless, they crystallization behaviour has not been studied yet.

The physical properties of polymer blends strongly depend on their crystallization behaviour and morphology. In a two component polymer blend, if the crystallization temperature of one component is higher than that of the other component, then the former crystallizes in the presence of the molten state of the other component, whereas the second component crystallizes in the presence of the solidified phase of the first component [13]. The presence of a second component either in the molten or solid state affects both the nucleation and crystal growth of the crystallizing polymer. Therefore, studying the morphology and crystallization of both components is desirable. Many articles have noted the effects of a second component on the crystallization of PP in PP [14–18]. Additionally, the majority of the practical manufacturing techniques of polymer composites (polymer and reinforcement) involve crystallization conditions that are analogous to non-isothermal crystallization.

The aim of the present work was to study the non-isothermal behaviour of biodegradable polymer/PP blends and to analyse the effect of the incorporation of compatibilizer and natural fibres. The studied materials can be used mainly in packaging applications with balanced costs and properties being very important to know the crystallization behaviour in order to design the processing steps.

Materials and methods

Materials

A biodegradable and biocompostable thermoplastic, Mater-Bi® (MB), based on polycaprolactone (PCL), thermoplastic starch, and additives (biodegradation time under controlled conditions: 20–45 days), with a degradation temperature around 420 °C, were kindly supplied by Novamont (Novara, Italy).

Isotactic polypropylene (PP), Moplen X30S (MFR = 8–10 g/10 min, Mw = 350,000 and Mn = 46,900), and polypropylene-graft-maleic anhydride (PP*) were supplied by Himont and Montell, Italy, respectively.

Hemp (*cannabis sativa*) fibres were kindly supplied by Sassetti Agricoltura S.R.L. (Bientina, Italy). In order to remove the non-cellulosic components, the fibres were first washed with liquid soap and immersed in 6 mass% NaOH solution for 24 h at 40 °C. The alkali treatment increases the number of free hydroxyl groups on the fibre surface and produces changes in the chemical composition by extracting lignin and hemicellulose [19]. After NaOH treatment, the fibres were repeatedly rinsed with distiled water, dried at 105 °C and finally stored for use.

Preparation of blends and composites

Blends of MB with PP and their composites with hemp fibres (MB/PP/H) were prepared in a Brabender Plasticorder internal mixer at a temperature of 175 °C. The mixing was carried out under nitrogen flux for 7 min using a rotor speed of 60 rpm. To increase the compatibility of the components in the system, PP* copolymer were added (2 mass%) to composites.

The composites were prepared by using a two-step mixing procedure: in the first step, masterbatches of MB with NaOH treated hemp (60/40 mass/mass) were processed in Brabender, then in the second step, 80 mass% of masterbatch was melt mixed with 20 mass% of polyolefin under the same conditions. In order to analyse the effect of compatibilizer on the morphology and final properties of blend and composite, 2 mass% of PP* was added to MB/PP matrix. All the examined systems are listed with their name in Table 1.

Scanning electron microscopy (SEM)

SEM analysis was carried out on the surfaces of samples cryogenically fractured in liquid nitrogen. The sample surfaces were sputter coated with a fine layer of gold in an Edward Sputter Coater and analysed by a Jeol JSM-5600LV scanning electron microscope. The sizes of dispersed polyolefin phases in blends were measured with semi-automatic software (Image Pro-Plus) from SEM micrographs.

Non-isothermal crystallization process (differential scanning calorimetric tests)

Non-isothermal crystallization tests were carried out in a Perkin Elmer Pyris 2 DSC. Pure indium was used as a

Table 1 Compositions and sample codes of examined materials

Sample name	Components	Compositions/mass%
MB	Mater-Bi	100
MB/PP	Mater-Bi/PP	70/30
MB/H	Mater-Bi/Hemp	68/32
MB/PP/H	Mater-Bi/PP/Hemp	48/20/32
MB/PP*/H	Mater-Bi/PP/PP-*g*-MAH/Hemp	48/18/2/32

reference material to calibrate both the temperature scale and the melting enthalpy. All DSC runs were performed under nitrogen atmosphere. Samples of approximately 10.0 ± 0.1 mg were placed in aluminum pans and loaded at room temperature to the DSC, heated up rapidly to 200 °C and maintained at this temperature for 2 min to remove thermal history. Then, the non-isothermal crystallization studies were carried out by cooling the samples down to 20 °C at several cooling rates: 5, 10, 20, and 30 °C min^{-1}.

Theoretical background

Modelling of non-isothermal crystallization process

The relative degree of crystallinity as a function of temperature, $x(T)$, can be calculated as:

$$x(T) = \int_{T_o}^{T} ((\partial Hc/\partial T)\mathrm{d}T) \Big/ \int_{T_o}^{T_\infty} ((\partial Hc/\partial t)\mathrm{d}T) \quad (1)$$

where T_o and T_∞ represent the onset and final crystallization temperatures, respectively; and H_c is the crystallization enthalpy.

It is well known that isothermal crystallization kinetics of polymers is commonly studied by the Avrami method [20]:

$$1 - x = \exp(-Z_t t^n) \quad (2)$$

where n is the Avrami crystallization exponent dependent on mechanism of nucleation, t is the time taken during the crystallization process, Z_t is a crystallization rate constant, and x is relative crystallinity of polymers at different temperatures. Both Z_t and n are constants which are denoted as a given crystalline morphology and type of nucleation at a particular crystallization condition [21]. Using Eq. (2) in double-logarithmic form

$$\ln(-\ln(1-x)) = \ln Z_t + n \ln t \quad (3)$$

By plotting $\ln(-\ln(1-x))$ versus $\ln t$ for each cooling rate, a straight line is obtained. From the slope and intercept of the lines, one can determine the Avrami's exponent n and the crystallization rate Z_t. Equation 2 is suitable for an isothermal crystallization system. Just like isothermal analysis, non-isothermal crystallization can be analysed by the Avrami equation, but, considering the non-isothermal characterization of the process investigated. Jeziorny [22] extended the isothermal Avrami's equation to the non-isothermal situation by proposing that the rate parameter, Z_t, should be corrected by cooling rate as follows:

$$\ln Z_c = \ln Z_t / \phi \quad (4)$$

where Z_c is the corrected kinetic rate constant and ϕ is the cooling rate.

A method developed by Mo [23] can be also employed to describe the non-isothermal crystallization process of semicrystalline polymers. Both Eqs. 3 and 4 can be related as follows:

$$\ln Zt + n \ln t = \ln K(T) - m \ln \phi \quad (5)$$

by rearrangement at a given crystallinity α, the equation is converted into:

$$\ln \phi = \ln F(T) - a \ln t \quad (6)$$

where $F(T) = [K(T) \cdot Z_t^{-1}]^{1/m}$ refers to the cooling rate, which must be chosen within unit crystallization time when the measured system amounts to a certain degree of crystallinity and $a = n \cdot m^{-1}$ is the ratio between the Avrami's to the Ozawa's exponent.

As it was described above, the crystallization temperature depends on the cooling rate. For non-isothermal crystallization, it is interesting to evaluate the effective energy barrier for the process that can be obtained by applying the differential iso-conversional method of Friedman that uses the following equation [24]:

$$\ln(\mathrm{d}x/\mathrm{d}t) = A - \Delta E_a / RT \quad (7)$$

where $\mathrm{d}x/\mathrm{d}t$ is the crystallization rate for a given relative crystallinity, A is an arbitrary factor and ΔE_a is the effective energy barrier of the process for a given relative conversion.

Thus, the relative crystallinity as a function of time, $\alpha(t)$, was differentiated to obtain the crystallization rate as a function of time. Then, by plotting $\ln(\mathrm{d}\alpha/\mathrm{d}t)$, measured at various cooling rate, against the corresponding inverse temperature for a given relative crystallinity, ΔE_a can be estimated from the slope.

Nucleation activity

Dobreva et al. [25] have developed an equation for calculating the nucleation activity (φ) of different substrates during the non-isothermal crystallization of polymer melts. If the reinforcement is extremely active, the nucleation

activity will tend to zero, while for inert reinforcement, it will be close to one. For nucleation from the melt, the cooling rate is represented by Eq. (8) at temperatures close to melting:

$$\ln(\phi) = A - (B/\Delta T_c^2) \quad (8)$$

where ϕ is the cooling rate, A is a constant, $\Delta T_c = T_m - T_c$ is the degree of subcooling, T_c is the temperature corresponding to the peak temperature of DSC crystallization, T_m is the melting temperature and B is a parameter related to the three dimensional nucleation. The value of B for the pure polymer and its composites (B^*) was obtained from Eq. (8). Then, φ can be calculated by Eq. (9)

$$\varphi = B^*/B \quad (9)$$

Results and discussion

SEM micrographs of fracture surfaces of the examined blends (with and without compatibilizer) are presented in Fig. 1. MB matrix and dispersed polyolefin phase appear as separated phases, due to the immiscibility of components. Blends MB/PP exhibited a characteristic droplet-like morphology with rather homogeneous size distribution. The micrographs of compatibilized systems indicated an improved phase dispersion and interfacial adhesion between polyolefins and MB. For MB/PP blends, it was found a remarkable effect of PP* incorporation on the average particle size which decreased from a value of about 28 μm for the uncompatibilized sample to about 12 μm for the sample with compatibilizer. SEM micrographs of fracture surfaces of composites with hemp showed weak interactions between matrix and fibres; for ternary composites, the dispersion of fibres and polyolefin in the matrix appeared almost uniform. The addition of compatibilizer contributed to reduce the particle size of dispersed polyolefin and improve the adhesion between fibre and matrix, as a consequence of interactions between the anhydride groups and hydroxyl groups of polysaccharide chains (i.e., starch and cellulose).The occurrence of such interactions has been reported for several polyolefin composites compatibilized with maleated PP [26–28].

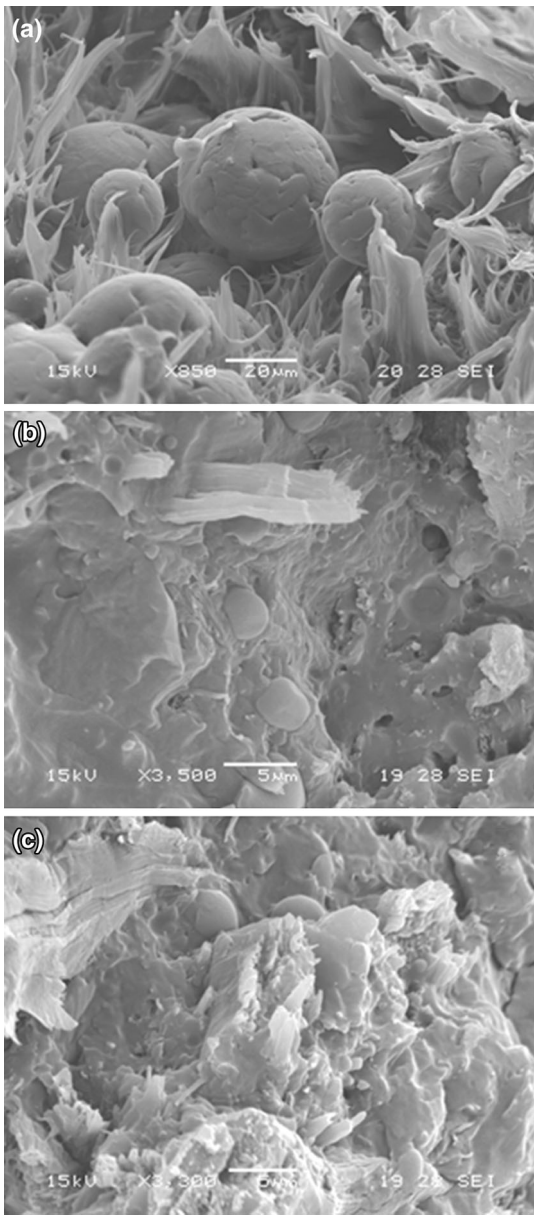

Fig. 1 Electronic micrographics by SEM for: (**a**) MB/PP, (**b**) MB/PP/H and (**c**) MB/PP*/H

Differential scanning calorimetric tests

The degree of crystallinity was calculated by using the following equation [29]:

$$X(\%) = \left(\frac{\Delta H_c}{w_l * \Delta H_{100}}\right) * 100 \quad (10)$$

where ΔH_c is the experimental heat of crystallization, w_l is the PP or MB mass fraction, and ΔH_{100} is the heat of crystallization of 100 % crystalline of PP (165 J g^{-1}) or the heat of crystallization of 100 % crystalline of PCL (136 J g^{-1}) [7, 30, 31].

Figure 2 show the crystallization behaviour of pure polymers and blends. From the previous figure, the values of crystallization temperature can be extracted and the obtained values are summarized in Table 2. Curves show two crystallization peaks, which indicate that these blends have two crystallizable components: PP at higher temperatures (around 111 °C) and MB at lower temperatures (around 46 °C). For MB/PP blends, both MB and PP components were able to crystallize at the cooling rates employed in the study. PP crystallized first and the

crystallization of MB occurred after complete crystallization of PP component. So, in the cooling conditions, when PP component was crystallizing, MB component was in the molten state, and the crystallization of MB occurred in the presence of PP crystals. Thus, the crystallization of PP component could be affected by amorphous MB and the crystallization behaviour of MB component will be influenced by the crystals of PP component [32].

Figure 3 show the T_c^{MB} (a) and T_c^{PP} (b) as a function of cooling rate. In both cases, the T_c decreased with increased cooling rate because the nuclei became active at lower temperatures [33], conducting to smaller spherulites during the heterogeneous nucleation process.

It is possible to observe that the crystallization temperature of PP (T_c^{PP}) increased with the incorporation of MB, indicating that the immiscible dispersed phase of MB acts as heterogeneous nuclei and PP starts to crystallize at a higher temperature [13, 32]. Dissimilar behaviour was observed in the crystallization temperature of MB (T_c^{MB}), where MB starts to crystallize at a lower temperature due to the presence of PP crystals [32].

By other hand, T_c^{MB} decreased when hemp fibres were added to the MB matrix, indicating a retardant effect. The same effect is observed in $T_c^{PP}$and T_c^{MB} when the hemp fibres are added to MB/PP blends. It may be due to hindrance physical of fibres to the motion of MB and PP chains [34].

Other studied effect is the incorporation of PP*. In that case, both, T_c^{PP} and T_c^{MB}, increased again approaching the values obtained in the system MB/PP. As it was previously mentioned, it was used in order to increase the compatibility of the components in the system. The polar groups of fibres react with maleic anhydride grafted in the PP and produce a more homogeneous blend or composite [35].

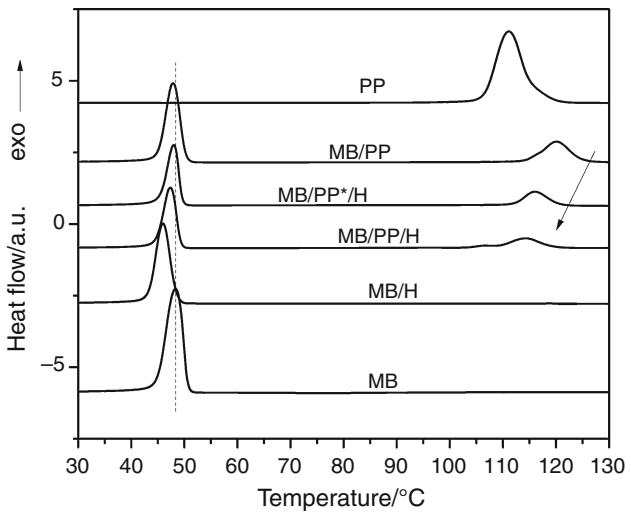

Fig. 2 Heat flow as a function of temperature at 10 °C min^{-1} for different samples during heating

The degree of crystallinity of MB was almost constant (62.5 ± 2.0 %) for the matrix and most composites, except in the case MB/H. The presence of fibres in the MB increases in a 5 % the crystallinity value. A similar value and tendency were found by other authors and was attributed to the possibility that the fibres acted as nucleating sites [36, 37]. By other hand, the degree of crystallinity of PP decreases in all systems with respect to PP matrix. The presence of fibres restricts the motion of PP chains; the restricted chains might not crystallize decreasing the crystallinity degree [38].

An approximation of the crystallization rate can be made by calculating the overall crystallization rate ($t_{1/2}^{-1}$, OCR), where $t_{1/2}$ (half-crystallization time) is the time at which the relative degree of crystallinity (α) approach to 0.5. A lower $t_{1/2}^{-1}$ value indicates slower crystallization. Figure 4 shows overall crystallization rate as a function of cooling rate for (4a) MB crystallization and (4b) PP crystallization. As expected, the value of OCR for MB and PP increased with the increased cooling rate for all materials. Table 2 presents the obtained values at 10 °C/min. It can be observed that for a fixed cooling rate, the OCR of PP ($t_{1/2}^{PP-1}$) increase when MB is mixed with PP, indicating that the addition of MB can accelerate the crystallization process (nucleating effect). The same behaviour is observed in $t_{1/2}^{MB-1}$. The OCR of PP and MB in the PP/MB blends decrease with the addition of fibres and increase with the use of PP*. As was previously justified, the fibres act as retard agent [34, 39], while the use of PP* favours the crystallization process, because a better interaction of the fibres with maleic anhydride grafted in the PP [40].

Modelling of non-isothermal crystallization process

The parameters of Avrami model (Avrami exponent, n, and rate constant, Z_c) were calculated in the range of x between 0.01 and 0.4, by to avoid the problems that arise due to the secondary crystallization [33]. The values of n obtained are summarized in Fig. 5 shown the parameters obtained as a function of cooling rate by the crystallization of MB and their blends (5a) and crystallization of PP and their blends (5b). The pure matrices present lowest values. In all cases, in the Fig. 5a, n decrease with the crystallization rate while in the case of the Fig. 5b, n is practically constant decrease to highest crystallization rate. Zou et al. [41] have reported that there are two factors which affect the value of n. One factor is that the fast crystallization rate of polymer at higher undercooling prevents the spherulites from their full development thereby lowering the value of n. Another one is that of growth site impingement, truncation of spherulites, and secondary crystallization which may change the crystallization mechanism.

Table 2 Parameters of non-isothermal crystallization for different materials studied at 10 °C/min

System	T_c^{MB}/°C	T_c^{PP}/°C	X^{MB}/%	X^{PP}/%	$1/1t_{1/2}^{MB}/s^{-1}$	$1/1t_{1/2}^{PP}/s^{-1}$
MB	48.3	–	64.4	–	0.028	–
MB/H	46.0	–	67.5	–	0.022	–
MB/PP*/H	47.9	116.0	60.5	48.0	0.028	0.015
MB/PP/H	47.6	114.7	62.2	48.4	0.019	0.012
MB/PP	47.8	120.1	62.3	56.7	0.032	0.012
PP	–	111.4	–	59	–	0.006

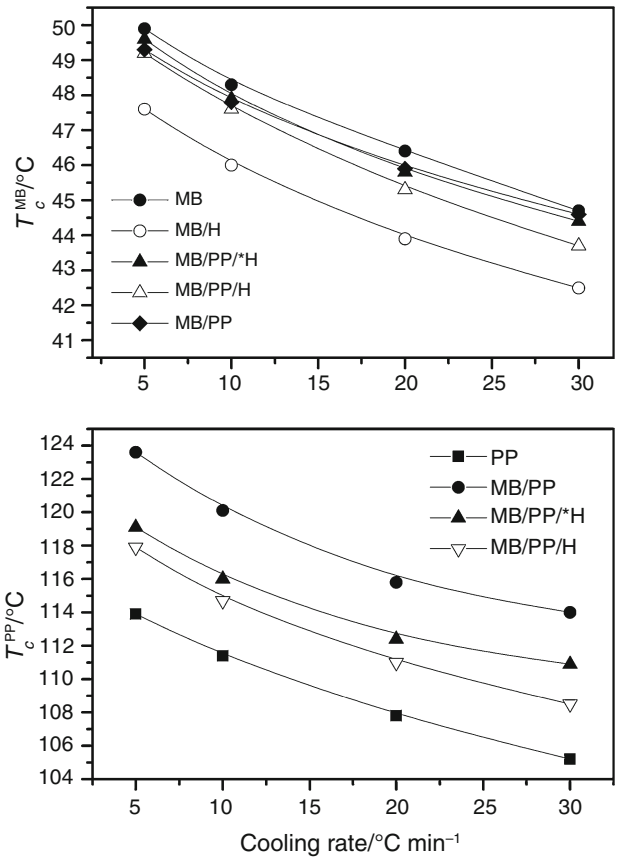

Fig. 3 T_C^{MB} (**a**) and T_C^{PP} (**b**) as a function of cooling rate

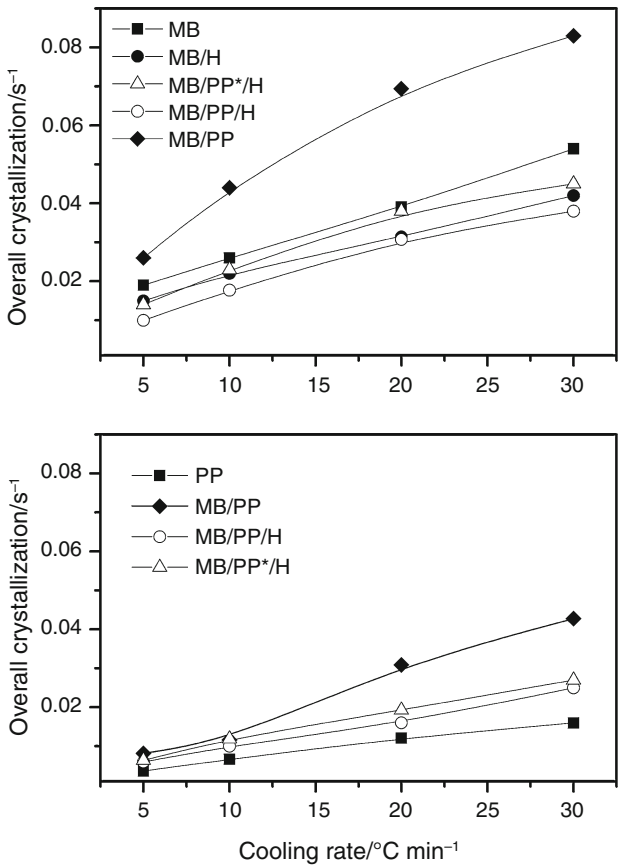

Fig. 4 Overall crystallization rate as a function of cooling rate for (**a**) MB Crystallization and (**b**) PP Crystallization

At a constant cooling rate in the MB crystallization (Fig. 5a), the variation in n value suggests that the fibres and the PP (alone and with PP*) exhibit different effects on the type of nucleation and crystal growth geometry of MB during crystallization. The average Avrami exponent n value of MB is close to 3 (at low cooling rate) indicating that crystallization process involves heterogeneous nucleation with spherulitic type growth [33]. The MB/PP and MB/H composites also present *n* values close to 3, but it increases when the three components are in the same composites, indicating that PP and H act as additional nucleating agents and lead to three dimensional spherulitic crystal growths [42]. As discussed earlier, the fibres retard the molecular mobility to reduce crystallization rate but also could act as nucleating agent to enhance the crystallization of MB [13]. By other hand, at a constant cooling rate in PP crystallization, the average value of n for neat PP and their blends with MB and H (Fig. 5b) is between 3.5 and 5.5. The largest value of n in the MB/PP blend is attributed to great nucleating effect of MB, as mentioned previously. The Avrami exponent $n > 4$ indicates a more complicated nucleation type and spherulite growth form [43].

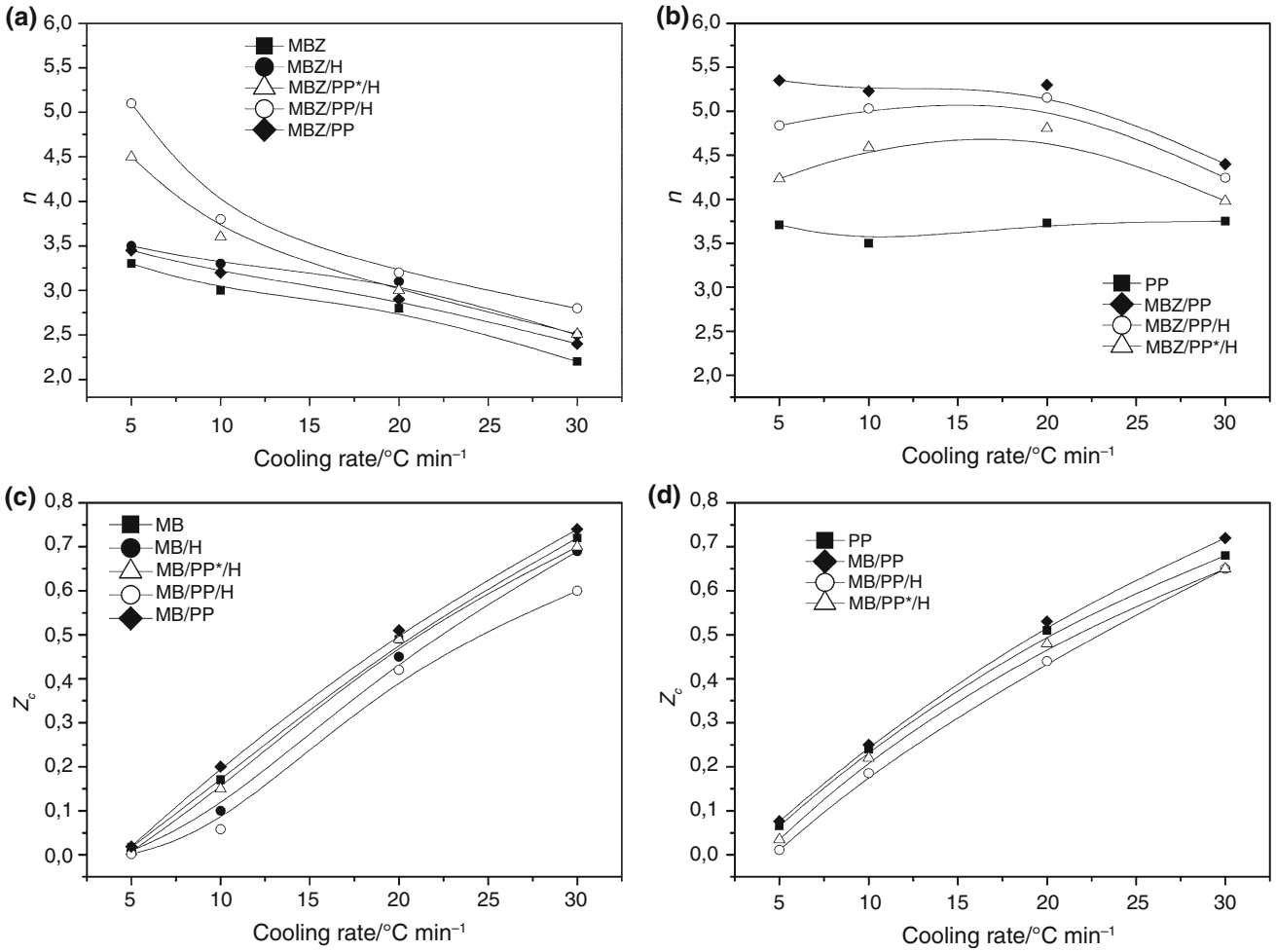

Fig. 5 Parameters of the Avramís model (n, Z_c) as a function of the cooling rate for (**a–c**) MB crystallization in MB/PP blends and (**b–d**) PP crystallization in MB/PP blends

Figure 5c, d shows the corrected crystallization constant (Z_c) in function of cooling rate for MB and PP crystallization, respectively. In both figures, Z_c increased as a function of cooling rate, which is an expected behaviour because it is an indication of the crystallization rate that gets faster under cooling [35, 44]. The crystallization rate of polymer depends upon the nucleation mode, nucleation density and the growth rate of individual crystallites [42]. In addition at a given cooling rate, the Z_c values were analysed in each case. In the Fig. 5c, when the fibres were added to MB, Z_c decrease indicating that it retarded the crystallization process. By other hand, Z_c increase in the system MB/PP (nucleating effect of PP) and decrease with the fibres. Finally, the system MB/PP*/H presents a greater Z_c value than MB/PP/H because PP* improves the system compatibility.

Figure 5d shows, at a given cooling rate, Z_c increase in the MB/PP system (by nucleating effect of MB) with respect to neat PP, decrease when the fibres are added and finally increase with the PP*. All model results are in agreement with the information discussed in previous section.

Table 3 shows the parameters obtained from Mo's model. These parameters (b and $F(t)$) were obtained by using the Eq. 5; by plotting ln ϕ versus ln t, the parameter $F(t)$ is obtained from slope and b from intercept. As it was previously indicated, values between 20 and 40 % of relative crystallinity were considered.

The values of $F(t)$ increased as a function of the relative degree of crystallinity. On the other hand, at a given degree of crystallinity, $F(t)$ present different behaviours. During the crystallization of MB, $F(t)$ decreased from 5.42 to 3.37 when the PP is added to MB, indicating that PP act as nucleating agent [35, 43, 44]. By other hand, when the fibre is added to MB, $F(t)$ increased showing a retarding effect [35, 45]. The same applies when the fibre is added to MB/PP system. The addition of PP* decreased $F(t)$, indicating a higher crystallization rate of MB/PP*/H system due to a higher crystallization rate of that system that could be attributed to the nucleation effect of PP* [40].

In the case of crystallization of PP, the effects are similar. $F(t)$ decrease with the addition of MB, increase

with the addition of fibres and crystallize faster ($F(t)$ decrease) with the use of PP*. In both cases, PP and MB crystallization, the b factor present the opposite effect.

As it was describe above, ΔE_a is the effective energy barrier of the process for a given relative conversion. The Eq. 7 is used for the sole purpose of making a qualitative comparison of the crystallization process between the polymers, since the equation was derived assuming a linear relationship between the crystallization rate, the crystallization constant and the conversion. In this work, ΔE_a was evaluated at a conversion of 0.3 and the values are reported in Table 4. In both cases, PP and MB crystallization, the activation energies decrease when PP is mixed with MB, indicating a nucleating effect of each component (MB when crystallize PP and PP when crystallize MB) and this is coincident with previous results. By other hand, ΔE_a increase when the fibres are added at the system MB/PP, and this is related with the hindrance physical of fibres to the motion of MB and PP chains, as was previously mentioned. The relative high values of activation energy, found in the presence of the fibres, could indicate a more ordered and organized structure of the transcrystalline layer of the nucleated matrix compared with the bulk of the neat matrix as it was demonstrated in previous studies [46].

Figure 6 presents the relationship between of $ln\ \varphi$ and ΔT^{-2} for calculating the nucleation activity in MB crystallization (Fig. 6a) and PP crystallization (Fig. 6b). As can be seen, a series of straight lines are obtained in both figures ($R^2 > 0.997$). Table 4 shows calculated values of the nucleation activity. In the MB crystallization, the values are lower in the systems MB/PP/H and MB/PP*/H by the double effect nucleating of PP and H, and is coincident with previous results. The effect is more notorious in the crystallization of PP, because MB presents a great nucleating effect during the crystallization of PP, but then

Table 3 Parameters from Mo's Model for all studied materials

Sample	X/%	Parameters from Mo's Model			
		b		$F(t)$	
		b^{MB}	b^{PP}	F^{MB}	F^{PP}
MB	20	1.22	–	5.42	–
	30	1.20	–	6.22	–
	40	1.24	–	6.80	–
MB/H	20	1.12	–	5.61	–
	30	1.11	–	6.32	–
	40	1.14	–	6.91	–
MB/PP*/H	20	1.30	1.26	5.10	5.75
	30	1.34	1.25	5.26	6.82
	40	1.37	1.23	5.58	7.54
MB/PP/H	20	1.28	1.08	6.17	9.39
	40	1.33	1.07	6.89	11.47
MB/PP	20	1.33	1.92	3.37	6.55
	40	1.36	1.77	4.16	9.30
PP	20	–	1.13	–	12.10
	40	–	1.11	–	14.38

Table 4 Activation energy (ΔE_a) for the transport of the macromolecular segments to the growing surface at a conversion of 0.3 and Nucleation activity obtained by Dobreva method

	Nucleation activity (φ)	$-\Delta E_a$/kJ mol^{-1}
MB crystallization		
MB	1	215
MB/H	0.87	298
MB/PP*/H	0.62	297
MB/PP/H	0.61	278
MB/PP	0.79	199
PP crystallization		
PP	1	253
MB/PP	0.35	239
MB/PP*/H	0.50	274
MB/PP/H	0.50	264

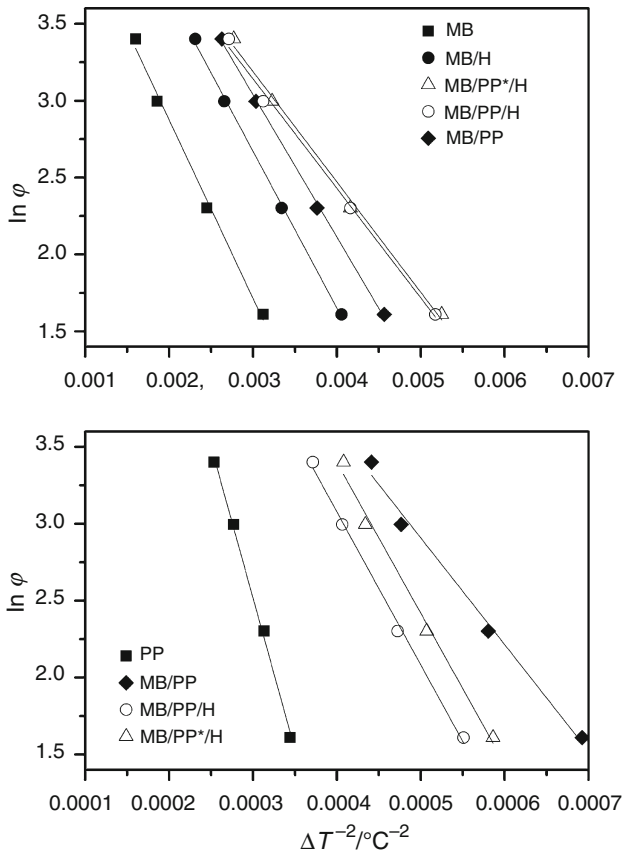

Fig. 6 Relationship between ln φ and $1/\Delta T_c^2$ for calculating the nucleation activity in (**a**) MB crystallization and (**b**) PP crystallization

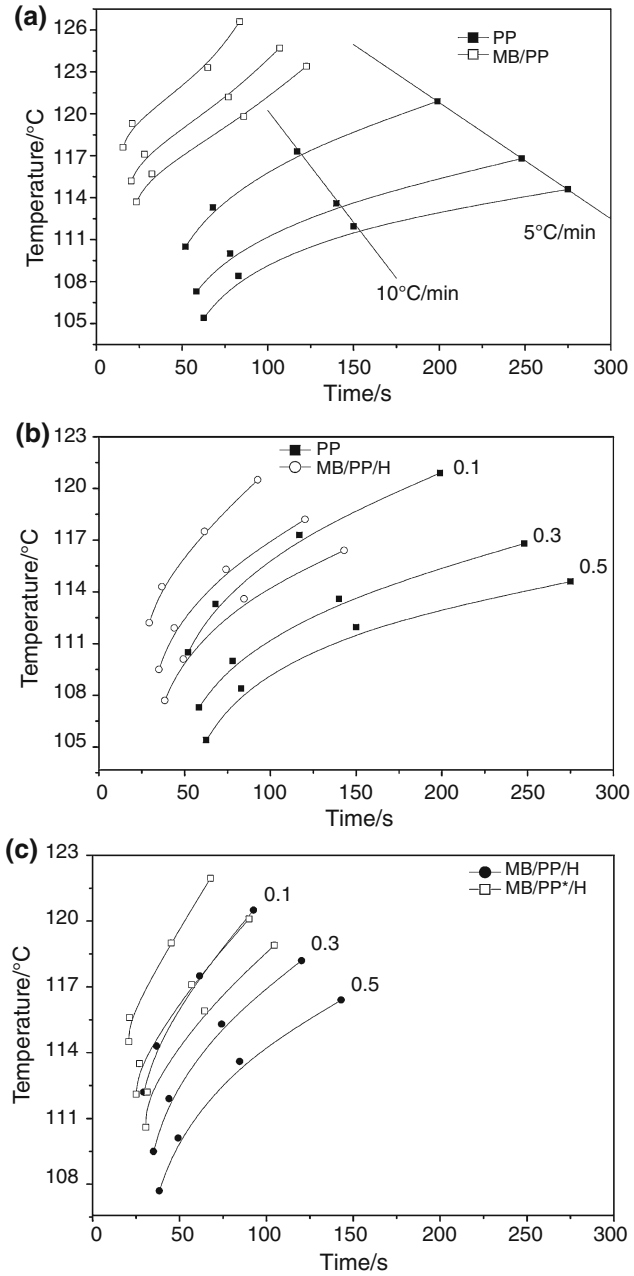

Fig. 7 CCT diagrams for PP crystallization for (**a**) PP and MB/PP, (**b**) PP and MB/PP/H (**c**) MB/PP/H and MB/PP*/H

decreased with the incorporation of fibres. The behaviour observed for the nucleation activity coincides with the evolution obtained with the n parameter from Avrami's equation.

Figure 7 shows the CCT, continuous cooling transformations, plots by the PP crystallization, where the crystallinity is related with time and temperature at a constant cooling rate. This approach allows the knowledge of the crystallization process [47, 48]. The curves for the relative degree of crystallinity (0.1, 0.3 and 0.5) are plotted as a function of time. Each point on these curves has been obtained by integration of the full model (nucleation and growth) at constant cooling rate. So, when the degree of crystallization curve (for example, by relative crystallinity at 0.3) is intercepted by a constant cooling rate one, the obtained point represents the time necessary to reach a specific relative degree of crystallization under specific thermal conditions. Fig. 7a reveals that the MB accelerate the crystallization process of PP (crystallize at higher temperature and in minor time) showing the nucleating effect observed previously. In the case of Fig. 7b, adding fibres to the MB/PP system, retards the crystallization process (larger times and lower temperatures) with respect to the MB/PP system. The last Fig. 7c shows the MB/PP/H and MB/PP*/H systems, indicating that the use of PP* accelerate the crystallization process by its compatibilizing effect. All results are in accordance with previous results. A similar behaviour was observed in the CCT plots corresponding to the MB crystallization.

Conclusions

The non-isothermal crystallization of biodegradable thermoplastic matrix (Mater-Bi®) and traditional thermoplastic (polypropylene) blends was studied using differential scanning calorimetry. Hemp fibres were used as filler, and maleic anhydride functionalized polypropylene was employed as compatibilizer.

It was showed that the molten MB act as nucleating agent to enhance the crystallization rate of PP and the solidified PP acted as nucleating agent to enhance the crystallization of MB. All experimental and models parameters results indicate that fibres retard the crystallization rate, whereas the PP* increased the crystallization rate.

The full model was used to order to build the CCT diagrams. These diagrams allow the determination of the crystallinity degree for different processing conditions. This information is very useful for the design and optimization of processing step. Besides, these diagrams confirmed the nucleating and retarding effect of different components in accordance with all previous analysis.

The calculation of the nucleation activity of the component, based on data from non-isothermal crystallization tests on cooling from the melt various rates, proved that in the MB crystallization the values are lower in the systems MB/PP/H and MB/PP*/H by the double effect nucleating of PP and H. By other hand, in the crystallization of PP, MB displayed a great nucleating effect during the crystallization of PP, but then decreased with the incorporation of natural fibres.

Acknowledgements The authors would like to acknowledge the financial support of the National Research Council of Argentina (CONICET) and the National Agency Promotion Scientific and Technological (ANPCyT).

References

1. Fang Q, Hanna M. Characteristics of biodegradable Mater-Bi®-starch based foams as affected by ingredient formulations. Ind Crop Prod. 2001;13:219–27.
2. Bastioli C. Biodegradable Materials. In: Brody AL, Marsh KS, editors. The Wiley encyclopedia of packaging technology. 2nd ed. New Jersey: Wiley; 1987. p. 77–83.
3. Bastioli C. Biodegradable materials state of art and future perspectives. Antalya: Frontiers in the Science and Technology of the Polymer Recycling; 1997.
4. Siracusa V, Rocculi P, Romani S, Dalla Rosa M. Biodegradable polymers for food packaging: a review. Trends Food Sci Technol. 2008;19:634–43.
5. Arcana M, Bundjali B, Yudistira I, Jariah B, Sukria L. Study on properties of polymer blends from polypropylene with polycaprolactone and their biodegradability. Polym J. 2007;39:1337–44.
6. Clarinval AM, Halleux J. Biodegradable polymers for industrial applications. In: Smith R, editor. Chapter 1. Elsevier Editorial. 2000. p. 1–29.
7. Haque MM, Alvarez V, Paci M, Pracella M. Processing, compatibilization and properties of ternary composites of Mater-Bi with polyolefins and hemp fibres. Compos A Appl Sci. 2011; 42:2060–9.
8. Pracella M, Pancrazi C, Haque MM, D'Alessio A. Thermal and microstructural; characterization of compatibilized polystyrene/natural fillers composites. J Therm Anal Calorim. 2011;103:95–101.
9. Pracella M, Haque MM, Alvarez V. Functionalization, compatibilization and properties of polyolefin composites with natural fibres. Polymers. 2010;2:554–74.
10. Mwaikambo LY, Ansell MP. Chemical modification of hemp, sisal, jute, and kapok fibres by alkalization. J Appl Polym Sci. 2002;84:2222–34.
11. Pracella M, Chionna D, Kulinski Z, Piorkowska E. Functionalization, compatibilization and properties of polypropylene composites with hemp fibres. Compos Sci Technol. 2006;66:2218–30.
12. Alvarez V, Mondragón I, Vázquez A. Influence of chemical treatments on the interfacial adhesion between sisal fibre and different biodegradable polymers. Compos Interface. 2007;14:605–16.
13. Huang JW, Wen YL, Kang CC, Yeh MY, Wen SB. Morphology, melting behavior, and non-isothermal crystallization of poly(butylene terephthalate)/poly(ethylene-*co*-methacrylic acid) blends. Termochim Acta. 2007;465:48–58.
14. Lin Z, Guan Z, Xu B, Chen C, Guo G, Zhou J, Xian J, Cao L, Wang Y, Li M, Li W. Crystallization and melting behavior of polypropylene in β-PP/polyamide 6 blends containing PP-g-MA. Ind Eng Chem. 2013;19:692–7.
15. Lin Z, Xu B, Guan Z, Chen C. Effects of polytrimethylene terephthalate on crystallization and melting behavior of beta-polypropylene in the blends. Ind Eng Chem. 2013;19:926–31.
16. Zhou H, Ying J, Liu F, Xie X, Li D. Non-isothermal crystallization behavior and kinetics of isotactic polypropylene/ethylene-octene blends. Part I: crystallization behavior. Polym Test. 2010;29:640–7.
17. Zhou H, Ying J, Liu F, Xie X, Li D. Non-isothermal crystallization behavior and kinetics of isotactic polypropylene/ethylene–octene blends. Part II: modeling of crystallization kinetics. Polym Test. 2010;29:915–23.
18. Tao Y, Mai K. Non-isothermal crystallization and melting behavior of compatibilized polypropylene/recycled poly(ethylene terephthalate) blends. Eur Polym J. 2007;43:3538–49.
19. Alvarez V, Ruseckaite R, Vázquez A. Mechanical properties and water absorption behavior of composites made from a biodegradable matrix and alkaline-treated sisal fibers. J Compos Mater. 2003;37:1575–88.
20. Avrami M. Kinetics of phase change. II Transformation-time relations for random distribution of nuclei. J Chem Phys. 1940; 8:212–6.
21. Wunderlich B. Macromolecular physics. New York: Academic Press; 1976.
22. Jeziorny A. Parameters characterizing the kinetics of the non-isothermal crystallization of poly(ethylene terephthalate) determined by d.s.c. Polymer. 1978;19:1142–4.
23. Liu TX, Mo ZS, Wang SG, Zhang HF. Nonisothermal melt and cold crystallization kinetics of poly(aryl ether ketone). Pol Eng Sci. 1997;37:568–76.
24. Vyazovkin S, Sbirrazzuoli N. Isoconversional analysis of calorimetric data on nonisothermal crystallization of a polymer melt. J Phys Chem B. 2003;107:882–8.
25. Dobreva A, Gutzow I. Activity of substrates in the catalyzed nucleation of glass-forming melts. II. Experimental evidence. J Non-Cryst Solids. 1993;162:13–25.
26. Feng D, Caulfiled DF, Sanadi AR. Effect of compatibilizer on the structure property relationships of kenaf fibre/polypropylene composites. Polym Compos. 2001;22:506–17.
27. Doan TTL, Gao SL, Mader E. Jute/polypropylene composites I. Effect of matrix modification. Compos Sci Technol. 2006;66: 952–63.
28. Majid RA, Ismail H, Taib RM. Effects of polyethylene-g-maleic anhydride on properties of low density polyethylene/thermoplastic sago starch reinforced kenaf fibre composites. Iran Polym J. 2010;19:501–10.
29. Yam WY, Ismail J, Kammer HW, Schmidt H, Kummerlöwe C. Polymer blends of poly(ε-caprolactone) and poly(vinyl methyl ether)—thermal properties and morphology. Polymer. 1999;40: 5545–52.
30. Nam PH, Maiti P, Okamoto M, Kotaka T, Hasegawa N, Usuki A. A hierarchical structure and properties of intercalated polypropylene/clay nanocomposites. Polymer. 2001;42:9633–40.
31. Ludueña L, Vázquez A, Alvarez V. Effect of lignocellulosic filler type and content on the behavior of polycaprolactone based eco-composites for packaging applications. Carbohydr Polym. 2012;87:411–21.
32. He YS, Zeng JB, Li SL, Wang YZ. Crystallization behavior of partially miscible biodegradable poly(butylene succinate)/poly (ethylene succinate) blends. Termochim Acta. 2012;529:80–6.
33. Di Lorenzo ML, Silvestre C. Non-isothermal crystallization of polymers. Prog Polym Sci. 1999;24:917–50.
34. Bin T, Qu JP, Liu LM, Feng YH, Hu SX, Chun Yin X. Non-isothermal crystallization kinetics and dynamic mechanical thermal properties of poly(butylene succinate) composites reinforced with cotton stalk bast fibers. Thermochim Acta. 2011; 525:141–9.
35. Perez CJ, Alvarez V. Overall crystallization behavior of polypropylene-clay nanocomposites; Effect of clay content and polymer/clay compatibility on the bulk crystallization and spherulitic growth. J App Pol Sci. 2009;114:3248–60.
36. Akos IN, Wyasu G, Ladan Z. Effect of fiber load and compatibilization on biodegradation of poly(ε-caprolactone)/poly(lactic acid) composites. Int Res J Mat Sci Eng. 2014;1:2–11.
37. Puglia D, Kenny JM, Santulli C, Sarasini F, Valente T. Thermal and mechanical characterization of phormium tenax reinforced polypropylene composites. J Thermoplast Compos Mater. Published on line February-2013. doi:10.1177/0892705712473629.

38. Mofokeng JP, Luyt AS, Tabi T, Kovacs J. Comparison of injection moulded, natural fibre-reinforced composites with PP and PLA as matrices. J Thermoplast Compos Mater. 2011;25: 927–48.
39. Zhou M, Li Y, He C, Jin T, Wang K, Fu Q. Interfacial crystallization enhanced interfacial interaction of poly (butylene succinate)/ramie fiber biocomposites using dopamine as a modifier. Compos Sci Technol. 2014;91:22–9.
40. Bouza R, Marco C, Ellis G, Martín Z, Gómez MA, Barral L. Analysis of the isothermal crystallization of polypropylene/wood flour composites. J Therm Anal Calorim. 2008;94:119–27.
41. Zou P, Tang S, Fu Z, Xiong H. Isothermal and non-isothermal crystallization kinetics of modified rape straw flour/high-density polyethylene composites. Int J Therm Sci. 2009;48:837–46.
42. Deshmukh GS, Peshwe DR, Pathak SU, Ekhe JD. Nonisothermal crystallization kinetics and melting behavior ofpoly(butylene terephthalate) (PBT) composites based on different types of functional fillers. Thermochim Acta. 2014;581:41–53.
43. Saengsuwan S, Tongkasee P, Sudyoadsuk T, Promarak V, Keawin T, Jungsuttiwon S. Non-isothermal crystallization kinetics and thermal stability of the in situ reinforcing composite films based on thermotropic liquid crystalline polymer and polypropylene. J Therm Anal Calorim. 2011;103:1017–26.
44. Alvarez V, Perez CJ. Gamma irradiated LDPE in presence of oxygen. Part I. Non-isothermal crystallization. Thermochim Acta. 2013;570:64–73.
45. Pengfei N, Xiaojun W, Baoying L, Shengru L, Jie Y. Melting and nonisothermal crystallization behavior of polypropylene/hemp fiber composites. J Compos Mat. 2011;46:203–10.
46. Klein N, Selivansky D, Marom G. The effects of a nucleating agent and of fibers on the crystallization of nylon 66 matrices. Polym Compos. 1995;16:189–96.
47. Pruiell J, White J. Structure development during polymer processing: Studies of the melt spinning of polyethylene and polypropylene fibers polym. Eng Sci. 1975;15:660–7.
48. Hsiung C, Cakmak M, White J. Structural gradients in injection molded poly-p- phenylene sulfide: influence of processing conditions and effect on mechanical behavior. Int Polym Proc. 1990;5:109–16.